The oxidation of styrene by chromium–silica heterogeneous catalyst prepared from rice husk

Farook Adam*, Anwar Iqbal

School of Chemical Sciences, Universiti Sains Malaysia, 11800 Penang, Malaysia

ARTICLE INFO

ABSTRACT

Chromium was incorporated into the silica matrix extracted from rice husk in basic, neutral and acidic medium. The prepared catalysts were labeled as RHCr-10, RHCr-7 and RHCr-3 according to their pH. The specific surface area of RHCr-10, RHCr-7 and RHCr-3 was determined to be 144, 143 and 564 $m^2 g^{-1}$, respectively. The XRD results showed the catalysts to be amorphous. RHCr-3 showed better catalytic activity with 99.92% conversion of styrene. Benzaldehyde was the major product with styrene oxide, phenyl acetaldehyde, acetophenone, 1-phenylethanol, phenylglyoxal, styrene glycol and benzoic acid as by-products. Leaching of chromium was minimal and RHCr-3 could be recycled several times.

© 2010 Elsevier B.V. All rights reserved.

1. Introduction

Paddy fields cover 1% of earth surface making it the second largest agricultural land use after wheat [1]. One of the major problems faced by this industry is the disposal of rice husk (RH). Even though RH has been used as fertilizer, heat insulator or as additive for cement and concrete fabrication, it will normally be burnt causing environmental and health issues [2–4]. Rice husk contains 20% ash, 38% cellulose, 22% lignin, 18% pentose and 2% other organic moieties [5]. The ash contains ca. 92–95% silica [6]. Recently, much research has been done on the potential use of the silica from rice husk as a support for heterogeneous catalysts. Controlled burning of RH can result in high purity silica at the same time eliminates the release of potentially toxic fumes into the atmosphere [7].

Chromium metal plays an important role in many industries. The catalytic activity of chromium mainly depends on its oxidation states. One major drawback in the use of chromium as heterogeneous catalyst is leaching. Laha and Gläser [8] had documented that considerable amount of chromium leached out during the oxidation of cyclohexanol when Cr–MCM-41 and Cr–MCM-48 were used as catalysts. Similar observation was also reported by Jha et al. [9] when Cr–MCM-41 was used in the oxidation of ethylbenzene and diphenylmethane. A few other authors also reported the similar phenomenon when chromium based heterogeneous catalysts were used [10,11].

Oxidation of styrene on the side chain draws interest from academics as well as the industry, mainly in the production of fine chemicals such as benzaldehyde. Normally, styrene oxidation will be carried out using stoichiometric amount of peracids such as peracetic and *m*-chlorobenzoic acid [12]. The usage of peracids leads to huge amounts of undesired products, is expensive and hazardous to handle while the usage of homogeneous catalyst such as methyltrioxorhenium (MTO) can cause equipment corrosion [13,14]. Heterogeneous catalyst together with greener oxidant like H_2O_2 and molecular oxygen had already started to draw attention from both modern chemical industry and academia in order to overcome these limitations. Zhang et al. reported that Mn–MCM-41 decomposes H_2O_2 very rapidly yielding to very low styrene conversion. They had also screened other metals such as Cr–MCM-41, Fe–MCM-41, Mo–MCM-41 and V–MCM-41 for the same conversion. They found that V–MCM-41 converted 20% of styrene but it could not be recovered due to leaching. When Cr–MCM-41 was used, the conversion was only 9.7%. Chromium species leached out from MCM-41 during the reaction until its physical appearance changed. The color of Cr–MCM-41 changed from orange to white after the reaction. However, no detailed explanations were given regarding this phenomenon [15]. Fe–MCM-41 and Mo–MCM-41 gave only 5.2 and 5.7% styrene conversion. Gómez et al. [16] tested the catalytic activity of Cr–MCM-48 in the oxidation of styrene. Chromium was incorporated into the MCM-48 support using ion exchange. Less than 5% chromium leaching was detected. The prepared catalyst managed to give 98% conversion in 24 h with benzaldehyde as a major product. However, no information was given on the recyclability of Cr–MCM-48.

* Corresponding author. Tel.: +60 4 6533567; fax: +60 4 6574854.
  E-mail addresses: farook@usm.my, farook_dr@yahoo.com (F. Adam).

In our previous reports, we successfully incorporated various transition metals by sol–gel method. The prepared catalysts showed good catalytic activity in the oxidation and benzylation reactions [17–20]. We also managed to functionalize silica with 3-(chloropropyl)triethoxysilane using the same method [21]. In this paper we report the synthesis of chromium incorporated rice husk silica at different pH. The catalysts were used to study the oxidation of styrene using hydrogen peroxide as the oxidant.

2. Experimental

2.1. Raw materials

Chromium(III) nitrate nonahydrate (Fluka, 97%) was used as a source of chromium. Other materials used were sodium hydroxide (Qrec), nitric acid (Qrec, 69%), m-xylene, cetyltrimethylammonium bromide (R&B), styrene (Merck) and acetonitrile (Lab Scan). All chemicals that were used are AR grade and were used as received. Rice husk (RH) was collected from a rice mill in Penang, Malaysia.

2.2. Extraction and modification of silica from rice husk (RH)

2.2.1. Pretreatment of RH
Rice husk was washed with tap water followed by distilled water to remove dirt. The washed husk was dried for 48 h at room temperature. 30.0 g of the dried husk was weighed and stirred with 750 mL of 1.0 M nitric acid for 24 h in a plastic container to reduce metallic impurities. The acid treated rice husk was washed thoroughly with distilled water until the pH of the rinse became constant. The rice husk was then dried at 383 K for 24 h.

2.2.2. Preparation of silica (RHSi-10, RHSi-7 and RHSi-3)
Silica extraction from RH was carried out by stirring the dried acid treated rice husk in 500 mL, 1.0 M sodium hydroxide for 24 h at room temperature. During the extraction process 0.01 mol of CTAB was added into the mixture. It was then filtered using Whatman No. 41 ash less filter paper. A brown colored mixture of sodium silicate was obtained. The sodium silicate was titrated with 3.0 M nitric acid at a rate of 1.0 mL min^{-1} with constant stirring until the solution pH reached either pH 10, 7 or 3. Gel started to form when the pH reached 10.5. The silica gel was aged for 24 h in the mother liquor. The gel was isolated by centrifugation and dried at room temperature for 24 h. In order to remove the surfactant, the xerogel formed was calcined at 773 K for 3 h. The silica obtained was grinded and labeled RHSi-10, RHSi-7 and RHSi-3.

2.2.3. Preparation of catalyst at different pH
The incorporation of chromium into the silica matrix was done following the same procedure as above except 10% of chromium salt (based on silica weight) was dissolved in ca. 50 mL of 3.0 M nitric acid and titrated first. This was followed by titration with 3.0 M HNO$_3$ until the required pH was reached. Green colored gel was formed. Recovering the chromium incorporated silica was done as in Section 2.2.2. The catalyst obtained was labeled RHCr-10, RHCr-7 and RHCr-3.

2.2.4. Sample characterization
The prepared samples were characterized by FT-IR (PerkinElmer System 2000) spectroscopy, N$_2$ adsorption porosimetry (Micromeritics Instrument Corporation model ASAP 2000, Norcross), powder X-ray diffractometry (Siemens Diffractometer D5000, Kristalloflex), scanning electron microscopy (Leo Supra 50 VP), energy dispersive spectrometry (EDAX FALCON SYSTEM), transmission electron microscopy (Philips CM12 Instruments). The UV–vis spectrum was obtained from a PerkinElmer Lambda

35 UV–vis spectrophotometer. AAS analysis was done using PerkinElmer AAnalyst 200.

Gas chromatograph analysis of the products was done using PerkinElmer Clarus 500 equipped with a capillary wax column (30 m length and 0.25 mm inner diameter) and FID detector. Products were identified using Clarus 600 GC–MS equipped with the same column.

2.3. Oxidation of styrene

The oxidation of styrene was performed in a 50 mL round-bottom flask. In a typical experiment, 10 mmol of styrene, 20 mL acetonitrile, and 100 mg of catalyst were mixed in the flask and heated to 353 K in paraffin oil. Then 40 mmol of dilute hydrogen peroxide (30%) was added to the flask. 1 mL aliquots of reaction mixture were withdrawn each hour. 5 μL of m-xylene was added to the withdrawn sample as internal standard before GC and GC–MS analysis. Leaching test was done using hot filtration technique according to the method described by Shylesh et al. [10] with a slight modification. The catalyst was removed after 30 min and the reaction was continued to completion. For recyclability test, the catalyst was separated followed by washing with hot solvent then dried at 383 K. This was followed by calcination at 773 K for 3 h to remove any adsorbed reactant or product molecules.

3. Results and discussion

3.1. The X-ray diffraction analysis

Fig. 1 displays the low and high angle XRD pattern of the catalyst. Low angle XRD pattern of RHSi-10 display one broad peak at $2\Theta = 2.21°$ and one small peak at $2\Theta = 3.37°$. The existence of these two peaks indicates a short range pore orders of mesoporous silica. In RHSi-7 and RHSi-3, these two peaks had flattened out. No peak was observed in low angle XRD pattern of RHCr-10, RHCr-7 and RHCr-3. High angle X-ray pattern of RHSi-10, RHSi-7 and RHSi-3 share one similarity with RHCr-10, RHCr-7 and RHCr-3 which is the existence of one strong broad peak around $2\Theta = 23°$ due to the amorphous nature of the silica material [22]. The absence of other peaks in RHCr-10, RHCr-7 and RHCr-3 indicates that the Cr$_2$O$_3$ crystals did not form on the surface. It also indicates that chromium species were homogeneously distributed on the silica matrix [9].

3.2. The nitrogen sorption analysis

All six samples exhibit type IV isotherm which is typical for mesoporous materials as shown in Fig. 2(a)–(f). RHSi-10 had IUPAC type H1 hysterisis loop. H1 hysterisis loop is characteristic of porous materials consisting of agglomerates or particles with uniform and regularly packed materials [23]. RHSi-7, RHSi-3, RHCr-10 and RHCr-7 exhibited IUPAC type H3 hysterisis loop. This is an indication of solids containing aggregates or agglomerates of particles forming slit shaped pores with non-uniform size and shapes [7]. RHCr-3 had a H2 hysterisis loop which is typical for an assemblage of various sized necks of ink bottle pores [24].

RHSi-10 had two types of pore sizes, i.e. between 17–23 and 76–113 Å in diameter as seen in Fig. 3(a). From Fig. 3(b), it can be seen that RHSi-7 had two types of pores as well. They were in the range of 33–43 and 79–145 Å. In RHSi-3, there was only one pore size ranging from 49 to 66 Å in diameter as shown in Fig. 3(c). The formation of bimodal porosity is directly related to the hydrolysis and condensation process of the silicon precursors. At high pH value, hydrolysis and condensation process was base-catalyzed and took place at a slower rate. In pH 10 and pH 7, the presence of NO$_3^-$ can shift the equilibrium of the surfactant and silicate assembly. NO$_3^-$ will block the adsorption of silicate ions on micelles and delay
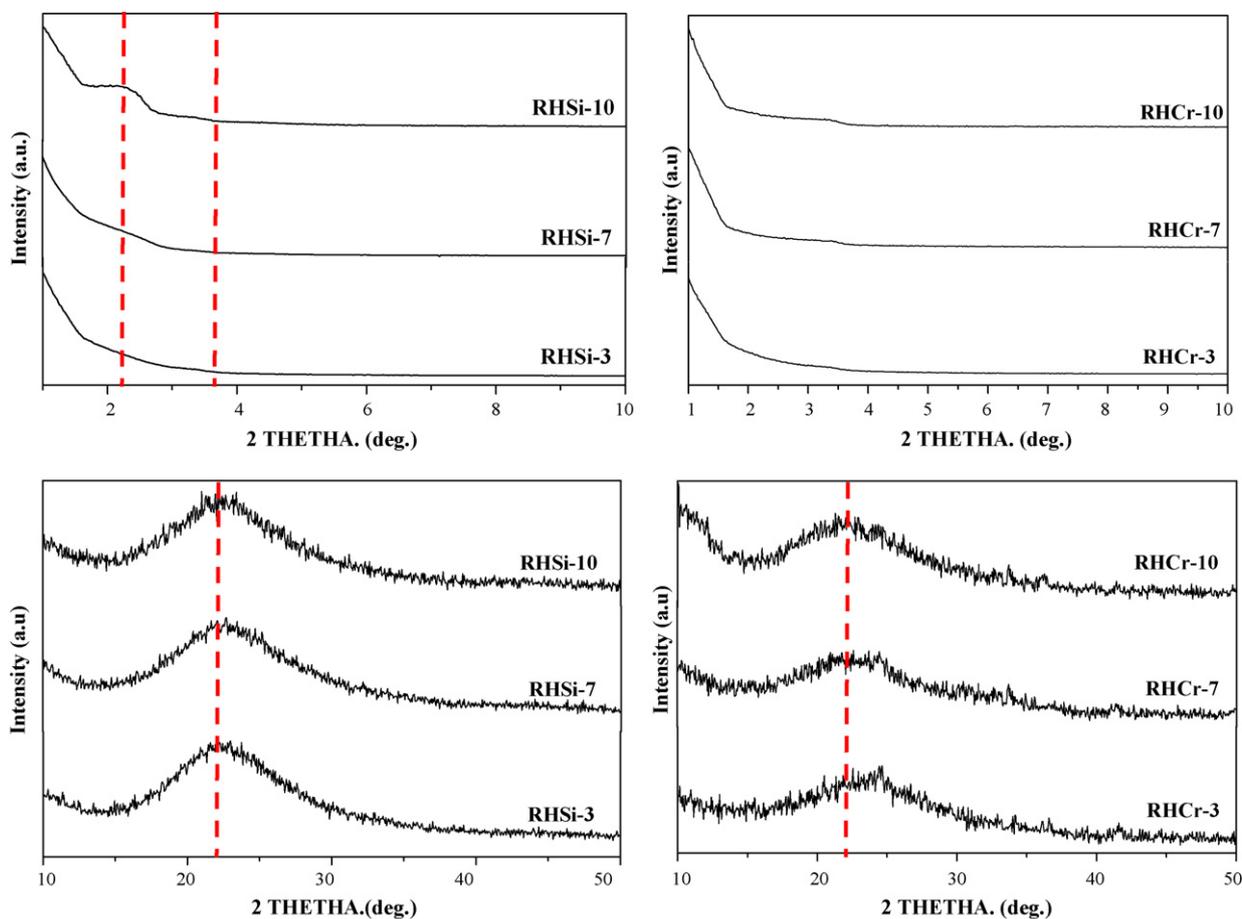
Fig. 1. The low and high angle X-ray diffraction pattern for the prepared catalyst.
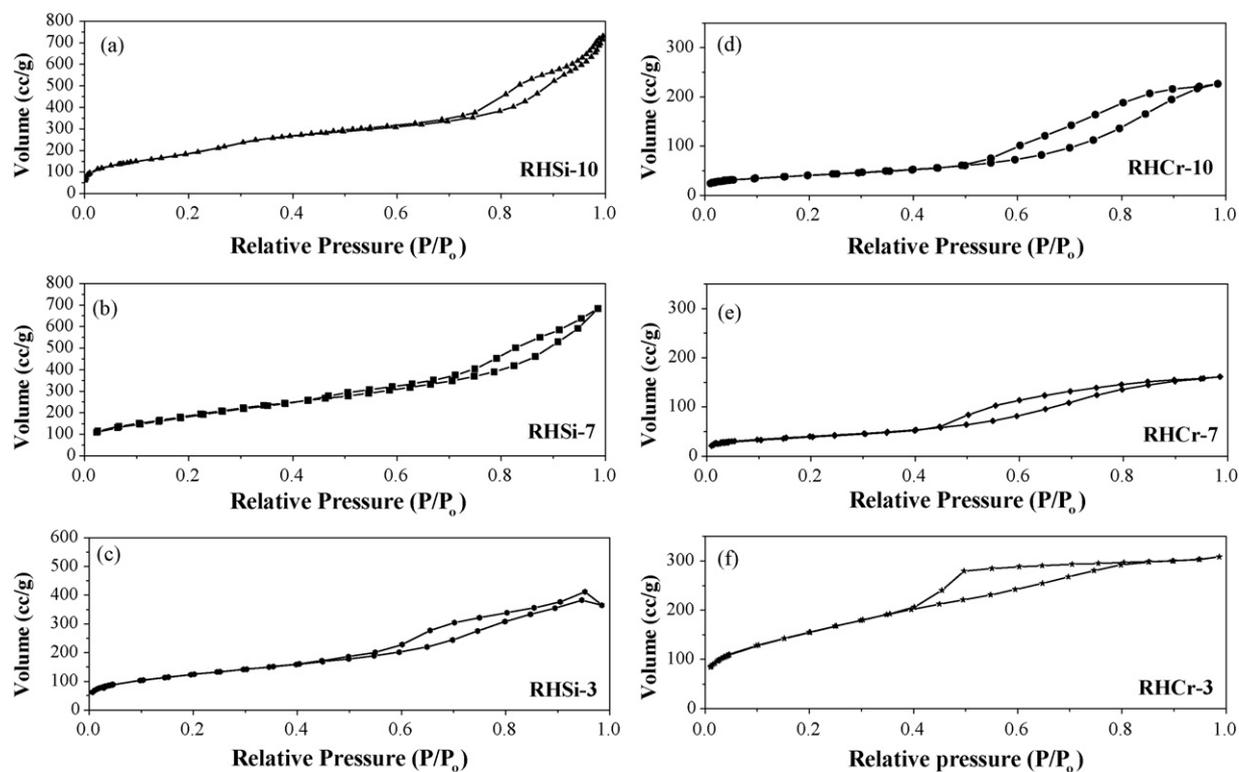

Fig. 2. The nitrogen sorption isotherm of (a) RHSi-10, (b) RHSi-7, (c) RHSi-3, (d) RHCr-10, (e) RHCr-7 and (f) RHCr-3.
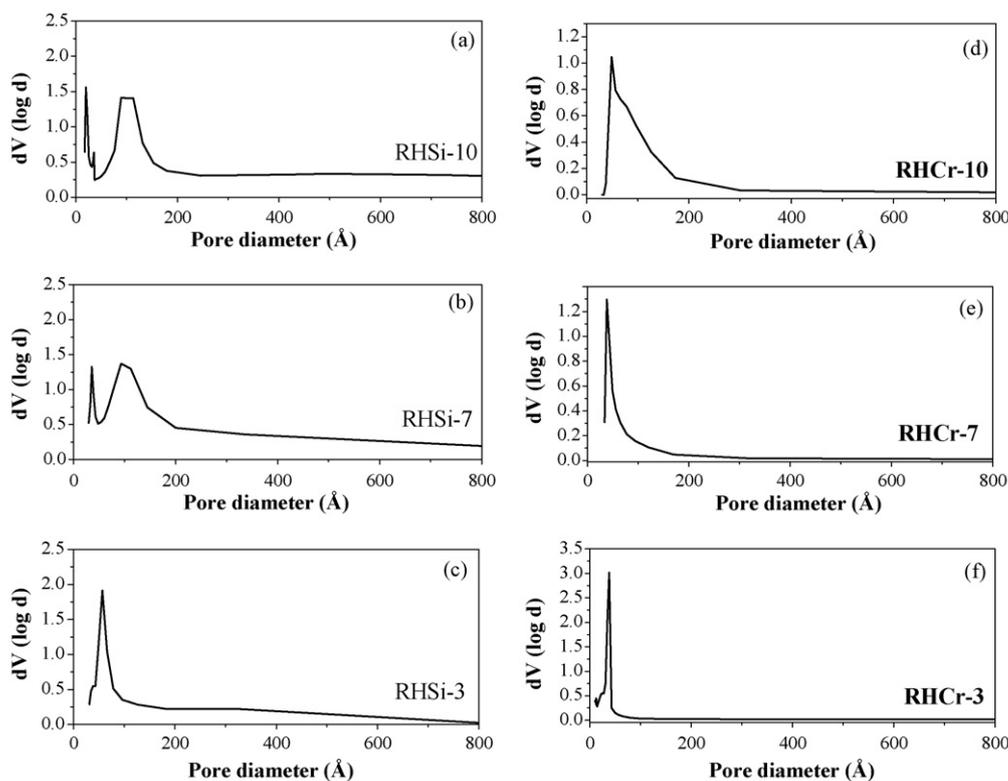
Fig. 3. Pore size distribution for (a) RHSi-10, (b) RHSi-7, (c) RHSi-3, (d) RHCr-10, (e) RHCr-7 and (f) RHCr-3.

the formation of the silica/surfactant mesophases. This can cause the incomplete interaction between silica species and surfactant, therefore smaller pores were formed by the template and the larger pore was formed by the agglomeration of silica nanoparticles during the hydrolysis–condensation [24,25] process. This could be the reason for the formation of bimodal pore system.

In acidic medium, the hydrolysis and condensation process was acid-catalyzed and took place at a faster rate. Near the isoelectric point of silica (pH 2), silica species are almost chargeless. Therefore, chargeless silica particles cannot directly combine with positively charged surfactant. For charge balance, there must exist a bridge counterion which is NO_3^- in this case at the interface of silica and surfactant. Bridging silica species with surfactant will increase the interaction between them thus completing hydrolysis and condensation process forming unimodal pore system [26] as observed for RHCr-3.

RHCr-10 had a pore size in the range of 43–126 Å (Fig. 3(d)), RHCr-7 had a pore size within 38–49 Å (Fig. 3(e)) and RHCr-3 had a pore range of 31–43 Å (Fig. 3(f)). The incorporation of chromium closed the smaller pores that existed in RHSi-10 and RHSi-7. The specific surface area for RHSi-10, RHSi-7 and RHSi-3 were 722, 700 and 445 $m^2\,g^{-1}$, respectively. However, the incorporation of chromium decreased the surface area: for RHCr-10 it was 144 $m^2\,g^{-1}$ while for RHCr-7 and RHCr-3 was 143 and 564 $m^2\,g^{-1}$, respectively. Chromium content was 7.26%, 4.91% and 2.34% in RHCr-10, RHCr-7 and RHCr-3, respectively. The amount of chromium loaded into the silica framework has a direct influence on the surface area of the catalysts. As the chromium content increased, the surface area decreased.

3.3. UV–vis diffuses reflectance analysis of the catalysts

The UV–vis diffuse reflectance spectrum for RHCr-10, RHCr-7 and RHCr-3 were obtained using potassium bromide as blank and is shown in Fig. 4.

After calcinations, RHCr-10 and RHCr-7 were yellowish indicating the presence of Cr^{6+} while RHCr-3 was green in colour indicating the presence of Cr^{3+}. The absorption band at ca. 460 nm was assigned to the charge transfer bands associated with the dichromate or polychromate species while bands at ca. 275 and ca. 375 nm could be assigned to the O to Cr(VI) charge transfer transitions of chromate species. The band at ca. 460 nm could also be due to the typical d–d transition corresponding to the $^4A_{2g}(F)$ to $^4T_{1g}(P)$ and $^4A_{2g}(F)$ to $^4A_{2g}(F)$ transitions due to the presence of the trivalent chromium ion, especially in RHCr-3. A small shoulder at ca. 610 nm could be due to the formation of nano-sized Cr_2O_3 [9,10]. However, the XRD patterns did not show this.
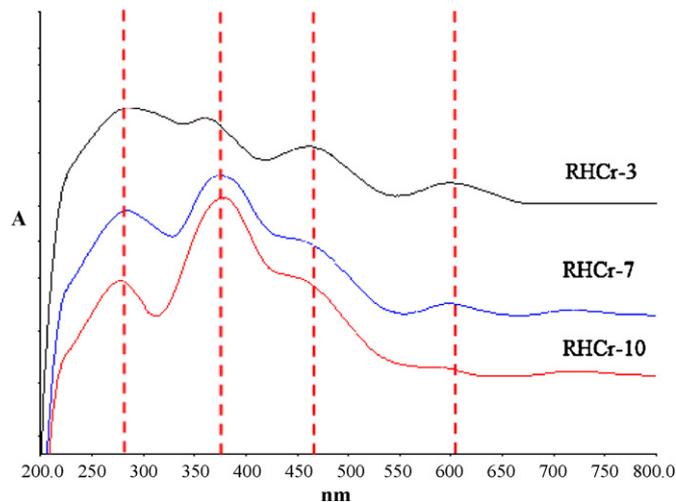

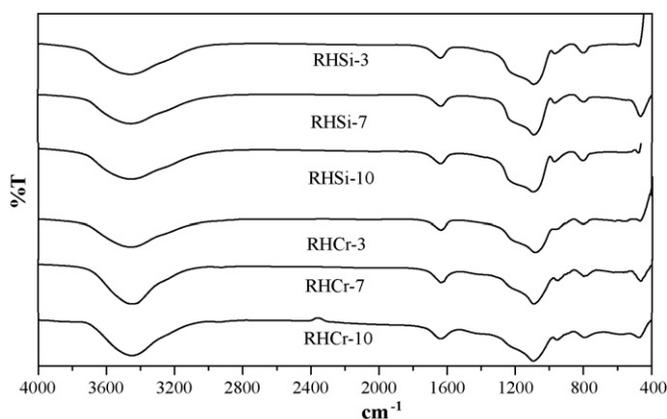**Fig. 4.** The UV–vis diffuse reflectance spectra of RHCr-10, RHCr-7 and RHCr-3.

Fig. 5. FT-IR spectra for the prepared catalysts.

3.4. EDX and AAS analysis

EDX analysis indicates the presence of silicon, carbon and oxygen in RHSi-10, RHSi-7 and RHSi-3. While in RHCr-10, RHCr-7 and RHCr-3, EDX analysis showed silicon, carbon, oxygen and chromium. Sodium was only detected in RHCr-10 and RHCr-7. From AAS analysis, the amount of chromium loaded in RHCr-10 was 7.26% while in RHCr-7 and RHCr-3 the loading was 4.91% and 2.34%, respectively. The percentage loading of chromium decreased with decrease in the pH.

3.5. FT-IR analysis

Fig. 5 is the FT-IR spectra for the prepared catalyst. The stretching vibration of SiO–H bond and the vibration of HO–H of water molecules adsorbed on the silica surface caused the appearance of a broad band around 3448–3456 cm^{-1}. The strong band at ca. 1637–1640 cm^{-1} was due to the bending vibration of water molecules. Asymmetric stretching vibration of the structural siloxane bond (Si–O–Si) was indicated by the strong band at ca. 1095 cm^{-1}. The band at ca. 802–807 and 468–479 cm^{-1} was attributed to symmetric stretching and bending modes of bulk Si–O–Si bond. The band at 971 cm^{-1} was attributed to Si–OH stretching vibration of the surface silanol groups. When chromium was loaded into the framework of silica, the band at 971 cm^{-1} shifted to lower wavelength, 949–956 cm^{-1}. The shift to the lower wave number is also an indication of possible superpose of the absorptions due to Si–O–Cr bonds [27].

3.6. TEM analysis

In RHSi-10, two types of morphologies can be seen as in Fig. 6(a). One is being rod like particles and the other one with ordered pore arrangements. A broad peak observed in RHSi-10 low angle XRD pattern was due to this short ranged pore orders. As the pH was reduced, RHSi-7 started to lose its pore arrangements but still maintained its porosity. This can be seen in Fig. 6(b). RHSi-3 did not show any existence of pore order as shown in Fig. 6(c). The incorporation of chromium metal into the silica matrix created a rather unique morphology. RHCr-10 has a lamellar structure. This might be due to the usage of CTAB as a surface directing agent and the formation of chromium nanocrystallites. Pore arrangements of RHCr-10 could not be seen clearly but the layers can be seen from the image in Fig. 6(d). TEM image of RHCr-7 in Fig. 6(e) has some similarity with TEM image of RHSi-7 in Fig. 6(b). Both images indicate high porosity. Fig. 6(f) is the TEM image of RHCr-3. RHCr-3 has a lamellar structured morphology similar to RHCr-10.

Table 1
The effect of preparation pH of catalyst on the product selectivity during oxidation of styrene.

Catalysts	Selectivity (%)							
	Bza	StO	PhAA	Ace	1-PHO	Pxal	Stycol	BA
RHCr-10	68.33	0.21	1.34	4.95	3.82	12.43	0.69	8.21
RHCr-7	68.87	0.24	1.17	5.38	3.75	11.36	0.67	8.56
RHCr-3	62.50	0	1.55	6.93	2.42	9.91	3.41	13.27

4. Oxidation of styrene

The optimum reaction conditions to achieve highest styrene conversion were determined by varying different parameters such as preparation medium, amount of oxidant, reaction temperature and amount of catalyst. The effect of each of these parameters on the oxidation of styrene is discussed in the following subsections. The main product detected was benzaldehyde (Bza), and the following compounds were detected as side products: styrene oxide (StO), phenylacetaldehyde (PhAA), acetophenone (Ace), 1-phenylethanol (1-POH), phenylglyoxal (Pxal), benzoic acid (BA) and styrene glycol (Stycol).

4.1. The influence of pH of catalyst preparation on the catalytic activity

The catalytic activity of RHCr-10, RHCr-7 and RHCr-3 was done using fixed amount of styrene (10 mmol), 100 mg of catalyst, 1:2 styrene to H$_2$O$_2$ molar ratio in 20 mL of acetonitrile. The reaction was carried out at 353 K for 6 h. As shown in Fig. 7, the amount of styrene converted was 86.99% when RHCr-3 was used. When RHCr-7 and RHCr-10 were used, the conversion was 77.85% and 71.81%, respectively. The conversion increased as the preparation pH of the catalyst was decreased. Bza was the main product in all cases. A small amount of StO was found when RHCr-10 and RHCr-7 was used. The product selectivity is shown in Table 1. From AAS, the amount of chromium loaded was higher in RHCr-10 and RHCr-7 compared to RHCr-3. High metal loading will reduce the surface area thus decreasing the catalytic activity of the catalyst. Although the metal loading in RHCr-3 was less than the other catalysts, it showed a higher conversion due to its higher surface area, and hence the larger number of active sites. Hence, RHCr-3 was used to optimize other parameters.

4.2. The effect of H$_2$O$_2$ on the catalytic activity of RHCr-3

The effect of H$_2$O$_2$ was demonstrated by considering four different compositions of styrene and H$_2$O$_2$ molar ratio, i.e. 1:1, 1:2, 1:3 and 1:4. The reaction was carried out at 353 K for 6 h using 100 mg of RHCr-3. As shown in Fig. 8, the conversion increased from 51.25% for 1:1 to 99.92% for 1:4. The catalytic properties of RHCr-3 in terms of product selectivity at different molar ratios are presented in Table 2. Bza was found to be the major product in all cases. The selectivity towards Bza decreased as the molar ratio of the reactants increased. StO was only found when 1:1 molar ratio was used. When the amount of H$_2$O$_2$ was increased, the production

Table 2
The effect of reactant composition on the selectivity during oxidation of styrene by H$_2$O$_2$ at different molar ratios of reactants (St = styrene).

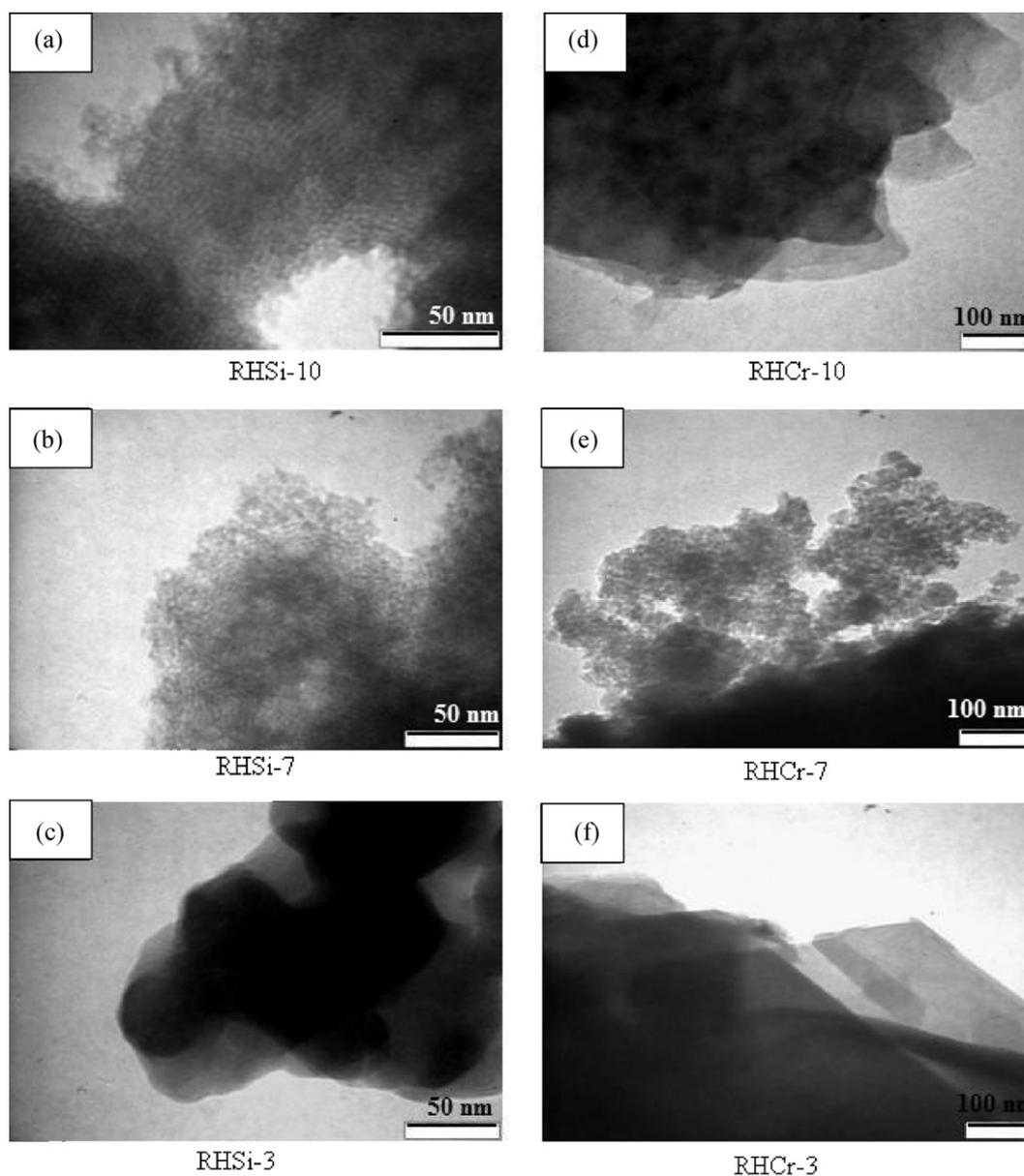| Molar ratio St:H$_2$O$_2$	Selectivity							
	Bza	StO	PhAA	Ace	1-POH	Pxal	Stycol	BA
1:1	72.17	0.48	1.89	5.52	4.98	9.2	0.63	5.13
1:2	70.89	0	0.79	6.42	4.85	9.8	0.15	7.11
1:3	62.5	0	1.55	6.93	2.42	9.91	3.41	13.27
1:4	63.07	0	2.49	4.32	1.45	9.21	1.68	17.78

Fig. 6. TEM images of (a) RHSi-10, (b) RHSi-7, (c) RHSi-3, (d) RHCr-10, (e) RHCr-7 and (f) RHCr-3.

of water as by-product increased as well. Water can increase the opening rate of the epoxide ring leading towards the formation of Stycol [28].

From Table 2, it can be seen that as the molar ratio of H_2O_2 increased, the formation of BA increased more than threefolds. This suggests that increasing the H_2O_2 results in the further oxidation of Bza to BA. Besides this, Stycol showed a fivefold increase when the molar composition was 1:3. Stycol could result from the hydrolysis of StO in the presence of excess H_2O_2 thereby effectively consuming all the StO that might have formed. Thus rendering StO not detectable at higher molar concentration of H_2O_2. All other by-products did not show significant variation as the molar concentration of H_2O_2 was increased. Thus 1:4 molar ratio was selected as the optimum ratio to achieve highest conversion.

4.3. The determination of the optimum reaction temperature for the catalytic oxidation of styrene

The oxidation of styrene was studied at three different temperatures, 303, 338 and 353 K, using 100 mg of RHCr-3 together with 1:4

styrene to H_2O_2 molar ratio for 6 h. The maximum styrene conversion of 99.92% was achieved when the reaction was carried out at 353 K. The results are shown in Fig. 9. The influence of temperature on the products selectivity is shown in Table 3. Selectivity towards Bza decreased as the temperature increased. Highest selectivity for Bza was 82.15% at 303 K. StO was formed at lower temperature. The selectivity for StO was 0.46 and 0.10% at 303 and 338 K, respectively. StO was not detected when the reaction temperature was increased to 353 K.

Table 3
The effect of reaction temperature on the product selectivity. Stycol and BA show an increase while Bza show a decrease as the reaction temperature was increased.

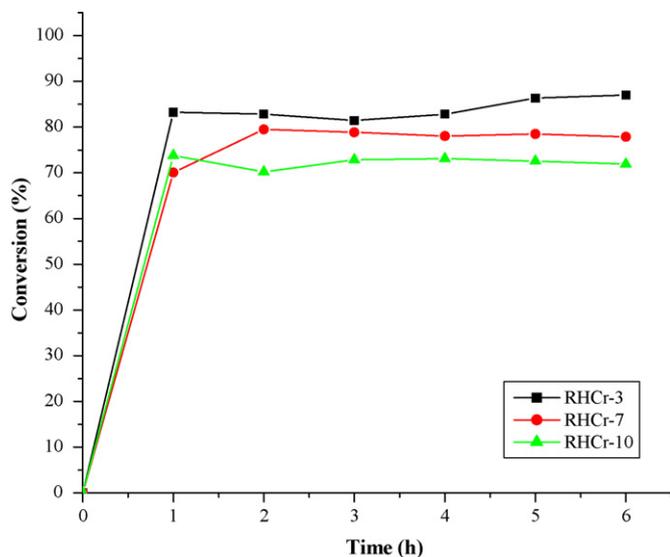| Temperature of reaction (K)	Selectivity (%)							
	Bza	StO	PhAA	Ace	1-POH	Pxal	Stycol	BA
303	82.15	0.46	1.66	1.64	0.69	7.57	0.39	5.43
338	73.81	0.10	1.19	4.39	2.53	10.16	0.24	7.57
353	62.5	0	1.55	6.93	2.42	9.91	3.41	13.27

Fig. 7. The effect of preparation pH of catalyst on the percentage conversion during oxidation of styrene by H_2O_2. 100 mg of catalyst was used with 1:2 styrene to H_2O_2 molar ratio. The reaction was carried out at 353 K.
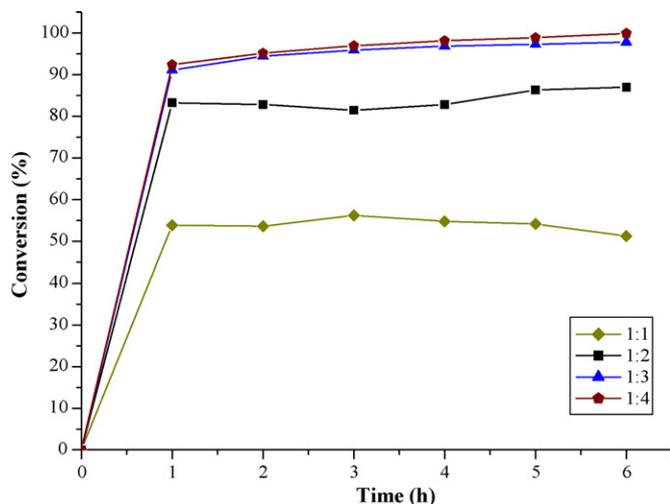

Fig. 8. The effect of reactant molar ratio on the percentage conversion during oxidation of styrene by H_2O_2. 100 mg of RHCr-3 was used and the reaction temperature was 353 K.
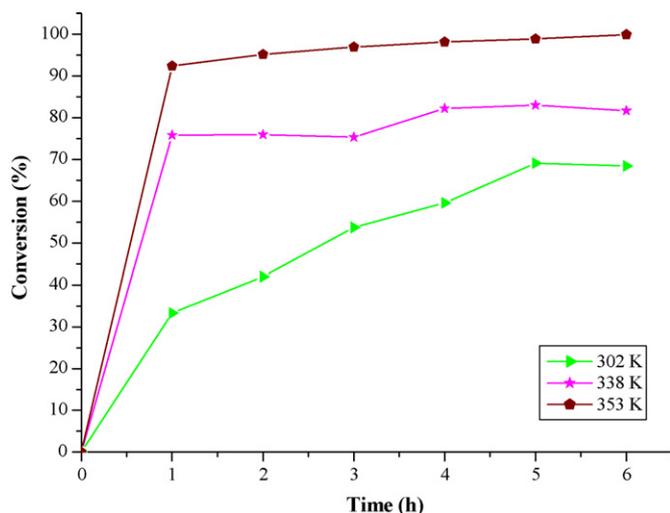

Fig. 9. The effect of reaction temperature on the percentage conversion of styrene. The mass of RHCr-3 used was 100 mg with a 1:4 molar ratio of reactants.
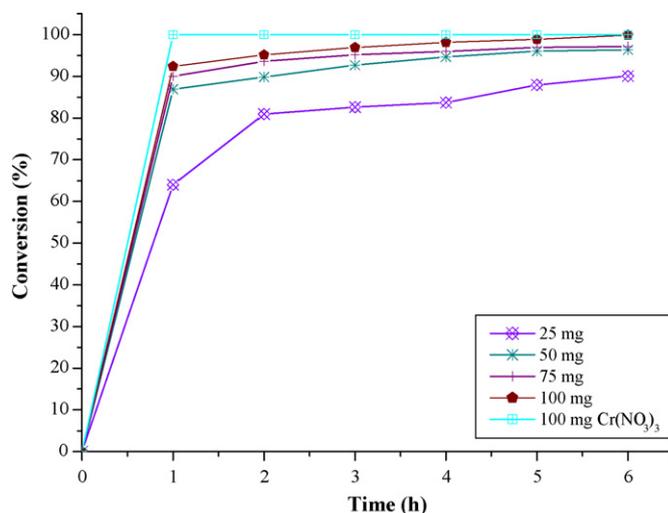

Fig. 10. The percentage conversion of styrene oxidation with different masses of RHCr-3 as the catalyst. 1:4 styrene to H_2O_2 was used and the reaction was carried out at 353 K. The catalytic activity of the homogeneous salt [$Cr(NO_3)_3 \cdot 9H_2O$, 100 mg] has been included for comparison.

It should be noted that Stycol and BA increased with reaction temperature. At temperatures lower than 353 K, StO was present. This shows that the StO was indeed formed during the reaction and subsequently converted to Stycol at higher temperatures. The decrease in Bza was at the expanse of the increase in BA as the temperature was increased. All other by-products did not show significant change with increase in reaction temperature. Subsequent studies were carried out at 353 K.

4.4. The optimum mass of catalyst for the oxidation of styrene

Different masses of RHCr-3 were used to determine the optimum conversion. The reaction was carried out using 1:4 styrene to molar ratio at 353 K. Fig. 10 shows the styrene conversion subjected to different masses of RHCr-3. A styrene conversion of 90.07% was obtained when 25 mg of RHCr-3 was used after 6 h. The conversion kept increasing until 99.92% with 100 mg of RHCr-3, after 6 h of reaction time in each case. However, the percentage conversion after the first hour with 25 mg of the catalyst was 64.02%, with 50 mg catalyst it was 86.92%, with 75 mg of the catalyst was 90.02% and with 100 mg catalyst it was 92.38%, respectively.

As the mass of catalyst increased, the selectivity towards Bza decreased progressively. The lowest selectivity of 63.07% for Bza was obtained when 100 mg of RHCr-3 was used. The product selectivity is shown in Table 4. StO was only detected when 75 mg of RHCr-3 was used, yielding 0.44%. However, this could be due to the presence of unconsumed StO. With other catalyst mass, StO was not detected as it could have been converted to other products, especially Stycol. With increasing mass of catalyst, the StO could have been converted to other products and thus escaped detection.

Table 4
The effect of the mass of RHCr-3 on the product selectivity.

Mass of catalyst (mg)	Selectivity (%)							
	Bza	StO	PhAA	Ace	1-PHO	Pxal	Stycol	BA
25	72.39	0	2.55	3.11	1.26	6.75	2.03	11.91
50	68.92	0	2.35	3.57	1.44	7.95	1.59	14.14
75	65.91	0.44	1.92	3.98	1.41	7.59	1.91	17.22
100	63.07	0	2.49	4.32	1.45	9.21	1.68	17.78
100[a]	64.82	0	1.52	5.05	1.30	5.67	0	21.62

[a] Reaction was carried out with $Cr(NO_3)_3 \cdot 9H_2O$ using the same optimum conditions for RHCr-3.

Increasing catalytic mass may also lead to the formation of other side products and decrease the Bza selectivity as indicated in Fig. 10 and Table 4.

Based on the parameters studied above, the optimum conditions to oxidize 10 mmol of styrene were found to be 40 mmol of H_2O_2 at 353 K for 6 h.

As a comparison, an additional homogeneous catalytic reaction was carried out using 100 mg of $Cr(NO_3)_3 \cdot 9H_2O$ under the optimum conditions. Within the first hour, 100% of styrene was converted into the products. Product selectivity obtained using $Cr(NO_3)_3 \cdot 9H_2O$ was similar with RHCr-3 as shown in Table 4. Selectivity towards Bza was 64.82%. It should be noted that StO and Stycol were surprisingly not detected with the homogeneous salt. Distribution of other products was similar to those obtained with RHCr-3. This comparison showed that RHCr-3 has the same catalytic behavior as the chromium salt in a homogeneous system with however, an added advantage that it can be separated and reused.

4.5. The effect of metal leaching and recyclability of RHCr-3 during oxidation of styrene with H_2O_2

Leaching study was carried out in order to determine the heterogeneity of RHCr-3 under the optimized conditions according to Shylesh et al. [10]. Even after the catalyst was removed, the conversion proceeded to 99.07% conversion suggesting possible chromium leaching during the initial stage of the reaction. The styrene conversion during leaching test is shown in Fig. 11.

The repeatability of RHCr-3 is shown in Fig. 12. The conversion dropped to 89.92% when the catalyst was recycled for the first time. During the second recycle, 93.54% of styrene was converted. When the catalyst was recycled for the third time, the conversion reduced to 85.05%. As the catalyst was recycled, selectivity towards Bza increased. StO was not detected at the end of the reaction. Product selectivity from the recyclability study is summarized in Table 5. No significant change in the product distribution was found in the recyclability test.

Observations based on the leaching test and recyclability test suggest that chromium leaching only happened during the first use and then stopped when RHCr-3 was recycled. Thus, it can be concluded that RHCr-3 becomes truly heterogeneous and stable after first use.
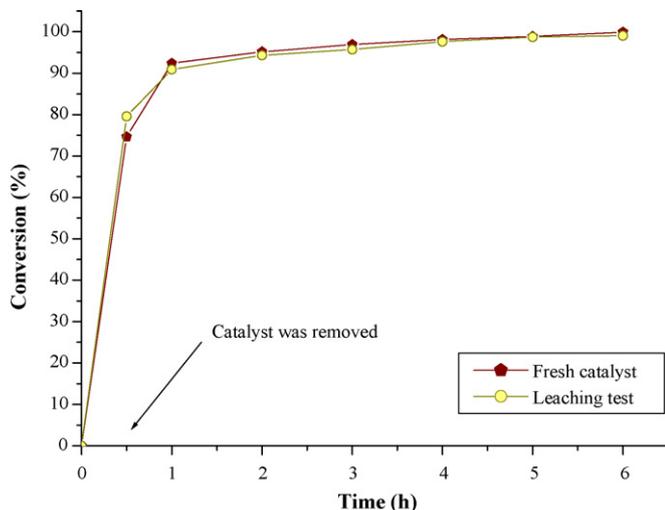

Fig. 11. The graph of percentage conversion of styrene during leaching test using fresh RHCr-3. The mass of catalyst used was 100 mg. Reaction temperature was 353 K and 1:4 molar ratio of reactants. The catalyst was removed after 30 min and the reaction allowed to continue to completion in 6 h.
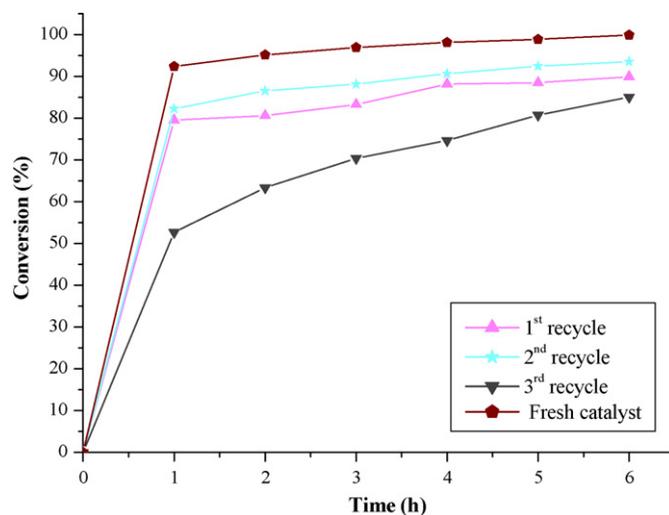

Fig. 12. The graph of percentage conversion of styrene with recycled RHCr-3 showing small loss in conversion. The mass of catalyst used was 100 mg. Reaction temperature was 353 K and 1:4 molar ratio of reactants.

Table 5
Product selectivity from recyclability test. The reaction was carried out at 353 K using 100 mg of RHCr-3 with 1:4 styrene to H_2O_2 molar ratio.

RHCr-3	Selectivity							
	Bza	StO	PhAA	Ace	1-POH	Pxal	Stycol	BA
1st recycle	75.16	0	2.96	4.55	1.39	2.89	0.35	12.69
2nd recycle	76.51	0	3.05	4.16	1.16	2.00	1.00	12.13
3rd recycle	79.28	0	2.82	3.73	1.03	2.11	0.67	10.37

Finally, the use of rice husk as the source of silica needs to be justified. In this regards it must be noted that silica extracted from rice husk is similar to commercial silica. Rice husk is a waste product and is freely available in most Asian countries. It also poses disposal problems due to its high silica content. Using rice husk as the source of silica gives added value to this waste material. Once silica is extracted from the rice husk, it becomes more amenable to biodegradation and eases the disposal problem. Compared to this, the use of TEOS [15,16] involves high cost. The manufacture of TEOS involves high temperature and pressure [29] and certainly raises environmental concerns. Substituting commercial silica precursor with silica extracted from rice husk will eliminate these problems. Besides that, it will also provide an alternative source of income for rice farmers. We also believe that the use of rice husk silica based catalysts will lead to cheaper and more environmental friendly catalysts. In short, it also addresses the call for green chemistry.

5. Conclusion

RHCr-3 showed better physicochemical characteristics and catalytic performance in the oxidation of styrene compared to RHCr-10 and RHCr-7. Highest styrene conversion was achieved when 100 mg of RHCr-3 was used together with 1:4 styrene to H_2O_2 molar ratio. Styrene conversion was 99.92% with 63.07% of selectivity to benzaldehyde when RHCr-3 was used. Catalytic performance of these catalysts relies on the surface area rather than the amount of chromium. Leaching of chromium ion was minimal and the reaction stayed essentially heterogeneous. The main product was Bza. Other side products detected were identified as StO, PhAA, Ace, 1-POH, Pxal and BA.

The advantages for the use of RHCr-3 catalysts over other reported chromium–silica catalysts are:

(i) Silica precursor used in this research is cheaper and prepared in a more environmental friendly manner compared to commercial silica used in most published work.

(ii) The preparation of RHCr-3 is cheap and did not require complicated procedures.

Acknowledgements

References

[1] J.L. Maclean, D.C. Dawe, B. Hardy, G.P. Hettel, Rice Almanac Source Book for the Most Important Activity on Earth, 3rd ed., CABI Publishing, Wallington, 2002.

[2] M. Nehdi, J. Duquette, A.E. Damathy, Performance of rice husk ash produced using a new technology as a mineral admixture in concrete, Cem. Concr. Res. 34 (2004) 521–526.

[3] V.P. Della, I. Kuhn, D. Hotza, Rice husk ash as an alternate source for active silica production, Mater. Lett. 57 (2002) 818–821.

[4] S. Chiarakorn, T. Areerob, N. Grisdanurak, Influence of functional silanes on hydrophobicity of MCM-41 synthesized from rice husk, Sci. Technol. Adv. Mater. 8 (2007) 110–115.

[5] F. Adam, K. Kalaivani, B. Saraswathy, Iron incorporated heterogeneous catalyst from rice husk ash, J. Colloid Interface Sci. 304 (2006) 137–143.

[6] R. Thankappan, S. Sugunan, Structural and catalytic investigation of vanadia supported on ceria promoted with high surface area rice husk silica, J. Mol. Catal. A: Chem. 250 (2006) 169–176.

[7] F. Adam, L.F. Cheah, Chromium modified silica from rice husk as an oxidative catalyst, J. Porous Mater. 16 (2008) 291–298.

[8] S.C. Laha, R. Gläser, Characterization and catalytic performance of [Cr] MCM-41 and [Cr] MCM-48 prepared by either classical or microwave heating, Micropor. Mesopor. Mater. 99 (2007) 159–166.

[9] R.K. Jha, S. Shylesh, S.S. Bhoware, A.P. Singh, Oxidation of ethyl benzene and diphenyl methane over ordered mesoporous M-MCM-41 (M = Ti, V, Cr): synthesis, characterization and structure–activity correlations, Micropor. Mesopor. Mater. 95 (2006) 154–163.

[10] S. Shylesh, C. Srilakshmi, A.P. Sigh, B.G. Anderson, One step synthesis of chromium-containing periodic mesoporous organosilicas and their catalytic activity in the oxidation of cyclohexane, Micropor. Mesopor. Mater. 99 (2007) 334–344.

[11] P. Branão, A. Valente, A. Ferreira, V.S. Amaral, J. Rocha, First stoichiometric large-pore chromium(III) silicate catalyst, Micropor. Mesopor. Mater. 69 (2004) 209–215.

[12] J. Song, Z. Zhang, T. Jiang, S. Hu, W. Li, Y. Xe, B. Han, Epoxidation of styrene to styrene oxide using carbon dioxide and hydrogen peroxide in ionic liquids, J. Mol. Catal. A: Chem. 279 (2008) 235–238.

[13] M. Selvaraj, S.W. Song, S. Kawi, Epoxidation of styrene over mesoporous Zr–Mn–MCM-41, Micropor. Mesopor. Mater. 110 (2007) 472–479.

[14] I.I. Misnon, Hidrophobic titanium oxide and gold loaded magnesium oxide aerogel catalysis in the oxidation of styrene, M.Sc. Thesis, Universiti Teknologi Malaysia, 2007.

[15] Q. Zhang, Y. Wang, S. Itsuki, T. Shishido, K. Takehira, Manganese-containing MCM-41 for epoxidation of styrene and stilbene, J. Mol. Catal. A: Chem. 188 (2002) 189–200.

[16] S. Gómez, L.J. Garces, J. Villagas, R. Ghosh, O. Giraldo, S.L. Suib, Synthesis and characterization of TM-MCM-48 (TM = Mn, V, Cr) and their catalytic activity in the oxidation of styrene, J. Catal. 233 (2005) 60–67.

[17] F. Adam, A.E. Ahmad, The benzylation of benzene using aluminium, gallium and iron incorporated silica from rice husk ash, Micropor. Mesopor. Mater. 118 (2009) 35–43.

[18] F. Adam, A.E. Ahmed, The benzylation of xylenes using heterogeneous catalysts from rice husk ash silica modified with gallium, indium and iron, Chem. Eng. J. 145 (2008) 328–334.

[19] F. Adam, A.E. Ahmed, Indium incorporated silica from rice husk and its catalytic activity, Micropor. Mesopor. Mater. 103 (2007) 284–295.

[20] F. Adam, P. Retnam, A. Iqbal, The complete conversion of cyclohexane into cyclohexanol and cyclohexanone by a simple silica–chromium heterogeneous catalyst, Appl. Catal. A: Gen. 357 (2009) 93–99.

[21] F. Adam, H. Osman, K.M. Hello, The immobilization of 3-(chloropropyl)triethoxysilane onto silica by a simple one-pot synthesis, J. Colloid Interface Sci. 331 (2009) 93–99.

[22] Y. Wang, Y. Ohishi, T. Shishido, Q.H. Zhang, W. Yang, Q. Guo, H. Wan, K. Takehira, Characterizations and catalytic properties of Cr–MCM-41 prepared by direct hydrothermal synthesis and template-ion exchange, J. Catal. 220 (2003) 347–357.

[23] F. Adam, S. Balakrishnan, P.L. Wong, Rice husk ash silica as a new support material for ruthenium based heterogenous catalyst, J. Phys. Sci. 17 (2006) 1–13.

[24] C.J. Brinker, G.M. Scherer, Sol–Gel Science: The Physics and Chemistry of Sol–Gel Processing, Academic Press, New York, 1990.

[25] X. Wang, W. Li, G. Zu, S. Qiu, D. Zhao, B. Zhong, Effects of ammonia/silica molar ratio on the synthesis and structure of bimodal mesopore silica xerogel, Micropor. Mesopor. Mater. 71 (2004) 87–97.

[26] H.P. Lin, C.Y. Mou, Acc. Chem. Res. 35 (2007) 192–201.

[27] R.S.D. Cruz, J.M.D.S.E. Silva, U. Arnold, U. Schuchardt, Catalytic activity and stability of a chromium containing silicate in liquid phase cyclohexane oxidation, J. Mol. Catal. A: Chem. 171 (2001) 251–257.

[28] V. Hulea, E. Dumitriu, Styrene oxidation with H_2O_2 over Ti-containing molecular sieves with MFI, BEA and MCM-41 topologies, Appl. Catal. A: Gen. 277 (2004) 99–106.

[29] W.L. Dai, H. Chen, Y. Cao, H. Li, S. Xie, K. Fan, Novel economic and green approach to the synthesis of highly active W-MCM41 catalyst in oxidative cleavage of cyclopentene, Chem. Commun. (2003) 892–893.